a GC and issues such as the presence of a central black hole (e.g. Lützgendorf et al. 2013, and references therein). This family of models has been successfully applied to ω Cen, 47 Tuc, and M 15 (Bianchini et al. 2013). In this thesis, we extend this sample, including the slowly rotating GC NGC 4372.

1.4 Deriving chemical abundances from stellar absorption lines

One of the main aims of the present work is to measure element abundances in GC stars in order to investigate the aforementioned questions pertaining GC formation. Thus, we will briefly introduce the basic principles of deriving chemical abundances from stellar spectroscopy. We measure the chemical composition of a star by analysing the absorption lines of different chemical elements in the stellar spectrum. The absorption lines are formed from the combined effect of an ensemble of atoms that absorb photons with a defined energy and thus decrease the intensity of the radiation field (bound-bound transitions). The stellar atmospheres contain mainly hydrogen (X $\sim$ 74%) and helium (Y $\sim$ 24%), and only traces of heavier elements (Z), typically $<$ 2% of the total mass per volume for Sun-like stars but the precise quantities can vary broadly in different stellar populations. Namely, the heavier elements are responsible for the majority of spectral lines we observe in the photospheres of cool stars. By measuring absorption lines in the stellar spectrum, we are able to infer the column number density of a particular absorber (responsible for the formation of the line of interest) along the line of sight. Most often the element abundance is given in logarithmic scale, relative to the Solar abundance – the square bracket notation ([A/B]):

$$[\mathrm{A/B}] = \log \frac{\mathrm{N_A}}{\mathrm{N_B}} - \log \frac{\mathrm{N_A^\odot}}{\mathrm{N_B^\odot}}, \tag{1.13}$$

where $\mathrm{N_A}$ and $\mathrm{N_B}$ are the column number densities of element A and element B in the star and the Sun, respectively. The column number densities are often given per 10^{12} hydrogen atoms. So, our goal is to derive the number of absorbing atoms responsible for the formation of a particular spectral line and then compute the total abundance of this element. Besides on the chemical abundance of the element, the intensity of the spectral lines depends on the physical conditions in the stars (e.g. effective temperature, gravity, microturbulence velocity) and on specific properties of the quantum transition (most importantly, the excitation potential and the oscillator strength of the transition). Generally, some quantum transitions are more probable than others. Transitions can be spontaneous or triggered by collisions or other environmental effects, such as electric and magnetic fields. The probability for a transition between two energy levels is determined by the Einstein coefficients: $\mathrm{A_{21}}$ gives the probability for a spontaneous emission, $\mathrm{B_{21}}$ gives the probability for a stimulated emission, and $\mathrm{B_{12}}$ gives the probability for a photo-absorption. The Einstein coefficients can be expressed as the net effect of an ensemble of quantum harmonic oscillators. Thus, the oscillator strength is a dimensionless quantity, which gives the effective number of quantum oscillators that have the same probability for a particular transition as the absorbing atom. To understand the impact of the physical conditions on the line intensity, we need to know which are the most probable/populated energy levels in the absorbing atom, what are the probabilities for transition, what is the relative number of atoms at different ionisation states, and what is the velocity distribution of the gas particles.

The electron distribution in the atoms is governed by a fundamental result of the statistical mechanics – higher energy levels are less probable than lower energy levels. The number of atoms in stellar atmospheres is so large that the probability distribution of different quantum states is practically equal to the number of absorbers. The number ratio of atoms in two energy levels

$E_b > E_a$ is determined by Boltzmann's equation:

$$\frac{n_b}{n_a} = \frac{g_b}{g_a} e^{-(E_b - E_a)/kT}, \tag{1.14}$$

$k = 1.38 \times 10^{-16}\,\mathrm{erg\,K^{-1}}$ is the Boltzmann constant, T is the gas temperature, and g is the statistical weight, which reflects the energy degeneracy of the different quantum states ($g_n = 2n^2$ gives the number of states that have energy E_n). Note that, according to the Boltzmann's equation, we need temperatures in the order of 85000 K to reach an equilibrium between the electrons on the first and second energy levels in the hydrogen atom but the Balmer lines (transitions from the second to higher energy levels) are strongest at temperatures around 10000 K, where we have much lower number of atoms in the first excitation state. To understand this, we have to look into the distribution of atoms at different ionisation states.

The number ratio of atoms at two different ionisation states n_i and n_{i+1} with ionisation energy χ_i is given by the Saha equation:

$$\frac{n_{i+1}}{n_i} = \frac{2u_{i+1}}{n_e u_i} \left(\frac{2\pi m_e kT}{h^2} \right)^{3/2} e^{-\chi_i/kT}, \tag{1.15}$$

where n_e is the electron density, h is the Planck constant, m_e is the mass of the electron, and u is the partition function. The partition function is the sum of possible energy states of the atom before and after ionisation. If E_n is the energy of level n, the partition function is defined as:

$$u = g_1 + \sum_{n=2}^{\infty} g_n e^{-(E_n - E_1)/kT}. \tag{1.16}$$

The factor of 2 in the Saha formula is due to the two possible spin numbers of the free electron. Half of the hydrogen atoms are ionised at a temperature ~ 9600 K and almost all of them are ionised at $T \sim 11000$ K, which explains the decrease of the Balmer lines intensity in hotter stars.

1.4.1 The line profile and spectral synthesis

Spectral synthesis is a common method for deriving chemical abundances. It requires proper modelling of the stellar atmospheres (the change of temperature, gas and electron pressure with optical depth, which govern the radiation transport) and understanding of the mechanisms that determine the intensity and shape of the absorption lines. The line profile is determined by $r_\lambda = F_\lambda / F_{cont}$, where F_λ is the flux in the line as a function of the wavelength and F_{cont} is the flux of the continuum. It contains a lot of information for the environment, in which the line forms. The opacity of the stellar atmosphere is highest in the centre of the line and decreases in the wings. In result, the centre of the line is formed in upper, cooler layers of the atmosphere, while the radiation from the wings reaches us from lower, hotter layers. There are three main processes that determine the broadening of the spectral lines:

• **Radiation damping**. The spectral lines have finite widths even in the idealised case when the atom is isolated and not in motion. This natural broadening is a consequence of the Heisenberg uncertainty principle $\Delta E \Delta t \sim h/2\pi$. The electrons remain a finite time Δt in excited states before leaving them. In result the energy levels are fuzzy (broadened). The ground state has the longest life time and is hence the least broadened. On the contrary, energy levels with high probability of transition are most affected by the radiation damping. The natural broadening is given by the following expression:

$$\Delta\lambda_E = \frac{\lambda^2}{2\pi c} \Gamma_{ik}, \tag{1.17}$$

where Γ_{ik} is the damping constant, which is defined by the Einstein coefficients for spontaneous radiation transitions. The line shape is determined by a Lorentzian profile with a width of $\Delta\lambda_E$.

• **Doppler broadening**. The atoms in the stellar atmosphere are in constant motion and their line of sight velocities cause an additional Doppler broadening of the line profile. For a gas in local thermodynamic equilibrium (LTE), the number of particles with a given velocity ($dn(v)$) in unit volume is constant and is described by the Maxwell-Boltzmann distribution:

$$dn(v) = \left(\frac{m}{2\pi kT}\right)^{3/2} e^{-mv^2/2kT} 4\pi v^2 dv, \tag{1.18}$$

where m is the mass of the particles. We can write the expression that determines the Doppler broadening using the Doppler effect and the most probable velocity $v_{mp} = \sqrt{2kT/m}$ according to to the Maxwell-Boltzmann distribution:

$$\Delta\lambda_D = \frac{2\lambda_0}{c}\sqrt{\frac{2kT\ln 2}{m}}. \tag{1.19}$$

Besides the thermal motion of the gas particles, there are also turbulent movements of large volumes of gas, especially in cool stars with convective envelopes. If the turbulent velocities on a micro-scale (microturbulence – the photons pass multiple gas cells before leaving the star) follow the Maxwell-Boltzmann distribution and their most probable velocity is v_{mic} we can write that

$$\Delta\lambda_D = \frac{2\lambda_0}{c}\sqrt{\left(\frac{2kT}{m} + v_{mic}^2\right)\ln 2}. \tag{1.20}$$

Since the projected on the line of sight Maxwellian distribution becomes Gaussian, the Doppler broadening is well described by a Gaussian profile with a width of $\Delta\lambda_D$. There might also be turbulent velocities on a macro-scale (macroturbulence) when the photons remain in a single gas cell from the time they are created until they leave the star. The net effect is a line broadening due to the convolution of multiple Doppler shifted spectra. The macroturbulence, however, does not change the line intensity.

• **Broadening due to particle collisions. Pressure effects.** The absorbing/emitting atoms are never isolated and the effect of the surrounding particles leads to an additional broadening of the lines - pressure effects. Common reasons for pressure broadening are the collisions between the particles. The transfer of energy from an excited atom to another particle shortens its average life-time and leads to additional broadening of the energy levels. The line profile is the same as the natural line profile and described by a Lorentzian profile with a width of $\Delta\lambda_c$ but the broadening can be much larger:

$$\Delta\lambda_c = \frac{\lambda^2}{2\pi c} n\sigma\sqrt{\frac{2kT}{m}}, \tag{1.21}$$

where σ is the cross-section of the collision and n is the particle density. The presence of charged particles around the absorbing atoms also causes broadening due to the inverse Stark effect and perturbation by van der Waals forces.

The Doppler broadening dominates the central regions of the line but when moving away from the central wavelength, its effect decreases quickly and the line wings are generally dominated by particle collisions and the radiation damping. Narrower lines are observed in the spectra of giant and supergiant stars due to the low density in their expanded atmospheres. The pressure effects are responsible for the broad lines in MS stars.

Most commonly, the spectral lines are modelled with a Voigt profile, which is a probability density function resulting from a convolution of a Gaussian (responsible for the Doppler broadening)

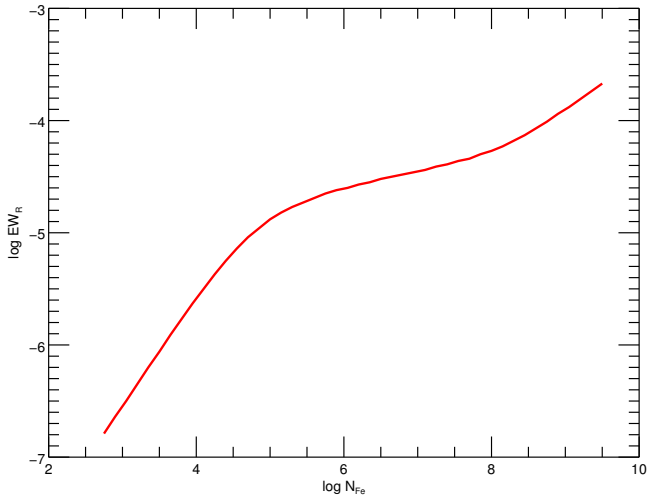

Figure 1.4: Curve of growth of the Fe I line at 5957 Å in a typical RGB star with $T_{\rm eff} = 4150$ K, $\log g = 0.9$ dex, and $v_{\rm mic} = 2.1$ km s^{-1}.

and a Lorentzian (responsible for the broadening due to particle collisions and radiation damping) profiles. Finally, the intensity of the spectral line is proportional to the number of absorbers, which we can estimate by fitting a synthetic line that takes into account all described effects to the observed spectrum. The total number of atoms of a particular chemical element can then be computed using the Boltzmann and Saha equations.

1.4.2 Equivalent widths and the curve of growth

A different approach to derive the chemical abundance from a stellar spectrum is to use the equivalent widths (EW) of the lines instead of synthesising their profiles. The latter can be computationally expensive and the line profiles can be very complex, modified by stellar rotation, macroturbulence, or motions of unknown origin. Furthermore, in reality, the observed line profile is a convolution between the intrinsic shape of the line and the spectrograph broadening function. With limited spectral resolution, a lot of the information encoded in the line profile is lost. The EW is an integral property of the line, which quantifies its intensity. It is defined as the width of a rectangle, which has the height of the continuum level and area equal to the area covered by the spectral line and is invariant to the above effects:

$$\mathrm{EW} = \int_{-\infty}^{+\infty} \frac{\mathrm{F_{cont}} - \mathrm{F_\lambda}}{\mathrm{F_{cont}}} \mathrm{d}\lambda. \tag{1.22}$$

The curve of growth determines the theoretical EW as a function of the number of absorbers. In Figure 1.4 we have plotted the rise of the reduced EW ($\mathrm{EW_R} = \log \mathrm{EW}/\lambda$) of the Fe I line at 5957 Å as a function of the Fe abundance. The reduced EW is a wavelength independent estimate of the strength of the line. When the number of absorbers is small, the EWs rise linearly with increasing the element abundance. As the number of absorbers continues to grow the optical depth at the central wavelength becomes increasingly larger and leads to saturation of the line. This means that there are no more available photons to excite the atoms and the curve of growth forms a slowly rising plateau ($\mathrm{EW} \propto \sqrt{\ln \mathrm{N_A}}$) governed by the still optically thin line wings. The further increase of the number of absorbers leads to a significant increase of the optical depth away from the central

wavelength and to the formation of strong damping wings coming from increasingly deeper layers. The EW starts to grow again following $EW \propto \sqrt{N_A}$.

In an explicit form the curve of growth for any transition can be written by integrating the line profile and substituting with the Boltzmann and Saha equations to get the full element abundance (Gray 1992):

$$\mathrm{EW_R} = \log \mathrm{C} + \log \mathrm{N_A} + \log \mathrm{gf}\lambda - \theta_\mathrm{x}\chi - \log \kappa_\nu, \tag{1.23}$$

where C is a constant specific for the star and the particular quantum transition, N_A is the number of atoms of element A relative to the number of hydrogen atoms, g is the statistical weight of the transition, f is the oscillator strength, $\theta_x = 5040/T$, χ is the excitation potential, and κ_ν is the continuum absorption coefficient. Note that a change of the elemental abundance is analogous to changes in the $gf\lambda$, $\theta_x\chi$, and κ_ν. Thus, curves of growth for different lines of the same species in the same star will only be shifted due to their individual χ, $\log gf\lambda$, and κ_ν but will have the same shape. Therefore, assuming we know the stellar atmosphere well, we can compute a generalised curve of growth for this star by adopting $\chi = 0$, $\log gf = 0$, $\lambda = \lambda_0$, and $\kappa_\nu = \kappa_0$ and vary only the abundance. Then, we can construct an empirical curve of growth by plotting the measured, reduced EWs of multiple lines of the same species against the known quantity $\Delta N_A = \log gf + \log(\lambda/\lambda_0) - \theta_x\chi - \log(\kappa_\nu/\kappa_0)$. A simple shift along the x-axis of the generalised curve of growth to the empirical curve of growth will give the real abundance of the element. The shape of the curve of growth is most significantly affected by the microturbulence, which tends to desaturate the spectral lines and is generally a free parameter in the abundance analysis. Generalised curves of growth incorporating different v_{mic} values can be then computed and the one that best describes the empirical curve of growth is considered representative for the star.

In practice, the atmospheric parameters are not well known. In this case a computation of a generalised curve of growth is not possible and we use an iterative procedure, where we derive the abundances from the individual curves of growth of all available lines by adopting a model atmosphere with effective temperature and gravity estimated from photometry, and empirical calibrations for the microturbulence velocity. Then the initial guess for the effective temperature is refined until all lines with different excitation potentials converge to the same abundance. The microturbulence velocity is inferred by removing any trend of the EWs of the various lines with the derived abundances. These steps are repeated until the derived abundances from all lines converge to a single value. Since the ionisation equilibrium is pressure sensitive, we can estimate the gravity by forcing the same abundance results from lines of different ionisation states of the element. If the distance to the star is known, however, as is the case with studying GCs, we can analyse separately neutral and ionised species, which should ideally converge to the same abundance. This is usually not the case due to departures from LTE (Heiter & Eriksson 2006; Lind et al. 2012; Bergemann et al. 2012), or an inappropriate choice of atmospheric models (e.g. using plane-parallel models, instead of spherical, or 3D models Bergemann et al. 2012).

Random errors arise from problems in measuring the EWs (e.g. blended lines) and poorly known atomic data but larger systematic errors come from uncertainties in the effective temperature (usually only known to a $100-150$ K precision), gravity, microturbulence, or inaccuracies in the model atmosphere. A way to deal with the poorly known atomic data is to perform a differential abundance analysis, where the EWs of the star of interest are directly compared to the EWs of a reference star with well known abundances and stellar parameters.

1.5 This thesis

The aim of this thesis is to study in detail the chemical and kinematic properties of Galactic GCs in order to put further constraints on their formation and evolution. We carry out detailed element